EXPERIMENTAL STUDY OF COHERENT STRUCTURES IN A TURBULENT BOUNDARY LAYER USING PIV

Michel Stanislas, Jean-Marc Foucaut, Jean-Philippe Laval, Lin Jie
LML UMR CNRS 8107
Bvd. Paul Langevin, Cité Scientifique
59655 Villeneuve d'Ascq
stanislas@ec-lille.fr

Johan Carlier
CEMAGREF - 17 Avenue de Cucill
CS 64429 - 35044 Rennes Cedex,
johan.carlier@cemagref.fr

ABSTRACT

Particle Image Velocimetry experiments have been performed in a turbulent boundary layer wind tunnel in order to study the coherent structures taking part in the generation and preservation of wall turbulence. The particular wind tunnel used is well suited for high resolution experiments ($\delta > 0.3$ m) at high Reynolds numbers (up to $R_\theta = 19\,000$ in the present results). The Particle Image Velocimetry experiments were carried out with different light sheet configurations including those similar to the visualization study by Head & Bandyopadhyay (1981). Eddy structures and near wall streaks were identified in instantaneous velocity maps in order to determine their mean characteristics.

INTRODUCTION

The aim of the present contribution is to study the near wall organization of a turbulent boundary layer. This organization was suggested fairly early by Theodorsen (1952) and has been since the subject of a tremendous amount of research which will not be summarized here. Although some points of agreement has emerged through the years, there are still points of controversy as is well illustrated by the review book by Panton (1997). In the present work, advantage was taken of the progress of PIV to provide good quality spatial data which allows presently to resolve the turbulence structures down to the Taylor microscales. These PIV data were recorded in different planes in order to try to asses at best the known coherent structures of the near wall region. These data were processed in the spirit of digital image analysis in order to extract quantitative data characterizing these coherent structures. Some of these data are presented hereafter and discussed compared to the literature.

EXPERIMENTAL FACILITY

The wind tunnel is 1×2 m^2 in cross section and 21.6 m in length. Transparent walls are used along the last 5 m of the working section on all sides to allow the use of optical methods. A return circuit is used to ensure a good control of the flow parameters. The temperature is kept within ± 0.2 C. The external velocity in the testing zone of the wind tunnel can be chosen continuously from 3 to 10 m/s with a stability better than 0.01%. The main characteristics of the boundary layer under study are summarized in table 1. These were obtained from HWA experiments carried out at $x = 19.6$ m from the inlet of the wind tunnel, that is about 2 m downstream of the location of the PIV experiments.

Table 1: Turbulent boundary layer characteristics

U_e (m s^{-1})	u_τ (m s^{-1})	δ (m)	δ^+ -	R_θ -	R_λ -
3	0.110	0.345	2 500	8 100	300
5	0.185	0.323	4 000	11 500	400
7	0.254	0.304	5 100	14 800	460
10	0.350	0.302	7 000	20 600	570

PIV APPROACH

In the present paper, the study is done using three series of PIV measurements: 2D2C PIV by Carlier (2001) and 2D3C PIV by Kähler & Stanislas (2000) and Jie et al (2004) taken in the same facility. These measurements give access to two or three components of the instantaneous velocity maps in various planes. Figure 1 illustrates the orientations of the various planes used in the three series of PIV measurements. One unit vector has been defined to characterize each coordinate $(\vec{e}_x, \vec{e}_y, \vec{e}_z)$. Two additional vectors $(\vec{e}_u, \vec{e}_d)$ are used to define simply two tilted planes (45^o upstream and 45^o downstream). The main characteristics of these measurements are summarized in table 2.

RESULTS

The vortices were detected in the instantaneous velocity map with an algorithm which is detailed in Carlier (2001) and Carlier (2001) and will not be described here. The algorithm to detect the streaks is briefly explained in the corresponding subsection.

Number of eddy structures

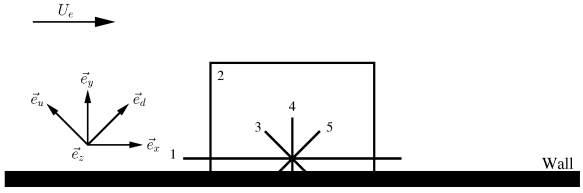

Figure 1: Orientations of the various planes used in the three series of PIV measurements: 1 $(\vec{e}_x, \vec{e}_z)$, 2 $(\vec{e}_x, \vec{e}_y)$, 3 $(\vec{e}_z, \vec{e}_u)$, 4 $(\vec{e}_z, \vec{e}_y)$, 5 $(\vec{e}_z, \vec{e}_d)$.

Table 2: PIV experiments characteristics

Plane configuration	$(\vec{e}_x, \vec{e}_y)$	$(\vec{e}_z, \vec{e}_y)$
PIV method	2D2C	2D3C
Field of view	$0.42^{\times} \times 0.28^{\times}$	$750^{+} \times 500^{+}$
Spat. res.	$0.0017^{\times} \times 0.0017^{\times}$	$5.5^{+} \times 5.5^{+}$
Number of R_θ	4	1
Number of maps	800	1565
Number of vectors	252×162	141×90

Plane configuration	$(\vec{e}_z, \vec{e}_u)$	$(\vec{e}_z, \vec{e}_d)$
PIV method	2D2C	2D2C
Field of view	$375^{+} \times 250^{+}$	$375^{+} \times 250^{+}$
Spat. res.	$4.1^{+} \times 4.8^{+}$	$4.1^{+} \times 4.8^{+}$
Number of R_θ	4	4
Number of maps	3200	3200
Number of vectors	94×54	94×54

Plane configuration	$(\vec{e}_x, \vec{e}_z)$
PIV method	2D3C
Field of view	$520^{+} \times 280^{+}$
Spat. res.	$5.2^{+} \times 4.7^{+}$
Number of R_θ	1
Number of maps	5000
Number of vectors	100×60

To give an order of magnitude, the mean number of eddy structures detected in each velocity map is about 6 in the $(\vec{e}_z, \vec{e}_u)$ plane, about 14 in the $(\vec{e}_z, \vec{e}_y)$ plane (the field of view is 4 times larger) and about 1 in the $(\vec{e}_z, \vec{e}_d)$ plane. To study the behavior of the number of eddy structures detected as a function of the wall distance, and to compare these data for various light sheet orientations, the wall distance was stratified in layers, each with a thickness of 24^{+}. The number of eddy structures having their centre in each layer is divided by the layer surface. The value obtained is called density of eddy structures in the layer.

Figure 2 presents this density for various plane orientations at $R_\theta = 7\,500$ and as a function of the wall distance. The identification method used did not allow to detect eddy structures with a centre lower than 40^{+} Carlier (2005).

In the $(\vec{e}_x, \vec{e}_y)$ plane, the two types of eddy structures ($\omega_o < 0$ and $\omega_o > 0$) are presented as they correspond to a different interpretation (no homogeneity hypothesis in that plane as in planes containing the z axis). It appears clearly in this plane that the eddy structures rotating in the natural

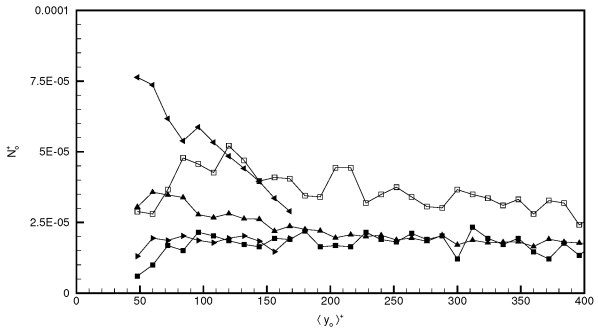

Figure 2: Density profiles of eddy structures in various planes at $R_\theta = 7\,500$: —□—, $(\vec{e}_x, \vec{e}_y)$ plane and $\omega_o < 0$; —■—, $(\vec{e}_x, \vec{e}_y)$ plane and $\omega_o > 0$; —▲—, $(\vec{e}_z, \vec{e}_y)$ plane; —◀—, $(\vec{e}_z, \vec{e}_u)$ plane; —▶—, $(\vec{e}_z, \vec{e}_d)$ plane.

sense ($\omega_o < 0$) are at least two times more numerous than the counter-rotating one ($\omega_o > 0$).

In the three transverse planes, only the eddy structures with the same sign of vorticity are presented. The $(\vec{e}_z, \vec{e}_u)$ plane shows clearly a peculiar behavior. The number of detected eddy structures is obviously increasing rapidly when approaching the wall. On the contrary, in the $(\vec{e}_z, \vec{e}_d)$ plane, the total number is much smaller and it decreases toward the wall. Also, the data in these two tilted planes are available only up to $y^{+} = 180$. Above this wall distance, an evolution toward some kind of equiprobability would lead the number of eddy structures in both tilted planes to converge toward the same value $({N_o}^{+} = (\mathrm{n/S})(\nu/\ u_\tau)^2 \simeq 2\ 10^{-5})$ around $y^{+} = 180$.

In the $(\vec{e}_z, \vec{e}_y)$ plane, the behavior is comparable to the $(\vec{e}_z, \vec{e}_u)$ plane; the number of eddy structures is again increasing toward the wall, but they are about two times less numerous as compared to the $(\vec{e}_z, \vec{e}_u)$ plane. Above $y^{+} \simeq 180$, based on a reasonable equiprobability hypothesis, one can expect all curves, except the one for $\omega_o < 0$ in the $(\vec{e}_x, \vec{e}_y)$ plane, to converge to the same and more or less constant value of ${N_o}^{+} \simeq 2\ 10^{-5}$. The region under investigation can then be separated into two sub-regions:

- Above $y^{+} = 180$, the number of eddy structures detected is the same in all planes except for $\omega_o < 0$ in the $(\vec{e}_x, \vec{e}_y)$ plane. These last eddies are more or less two times as numerous as the others and their population is slowly decreasing with the wall distance (while the others remain relatively constant in the field of view). The fact that the number of $\omega_o < 0$ eddy structures is about two times the number of eddy structures of one sign in the $(\vec{e}_z, \vec{e}_u)$ and $(\vec{e}_z, \vec{e}_y)$ planes indicates that statistically one head is more or less associated to one leg (of either sign) in this region, thus arguing more in favor of the cane hypothesis that the hairpin one.

- Between $40 < y^{+} < 180$, the situation is a bit more complex. The number of eddy structures detected in the $(\vec{e}_z, \vec{e}_u)$ plane increases rapidly toward the wall, while the number in the $(\vec{e}_z, \vec{e}_d)$ plane is nearly constant and finally decreases very near to the wall. This result supports the hypothesis that the eddy structures in this region are

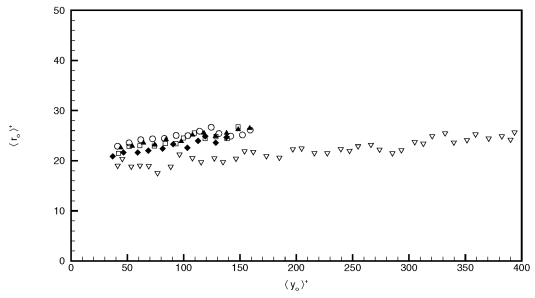

Figure 3: Mean radius profiles of eddy structures: ▽, $(\vec{e}_x, \vec{e}_y)$ plane and $R_\theta = 7\,500$; ♦, $(\vec{e}_z, \vec{e}_u)$ plane and $R_\theta = 7\,500$; □, $(\vec{e}_z, \vec{e}_u)$ plane and $R_\theta = 10\,500$; ▲, $(\vec{e}_z, \vec{e}_u)$ plane and $R_\theta = 13\,500$; ◯, $(\vec{e}_z, \vec{e}_u)$ plane and $R_\theta = 19\,000$.

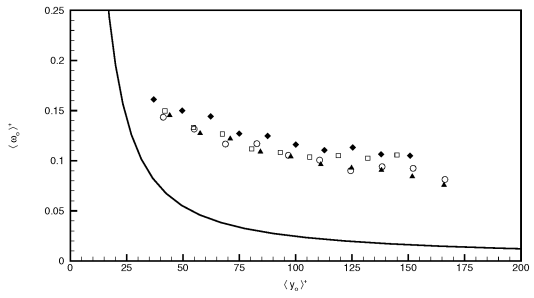

Figure 4: Mean vorticity profiles of eddy structures: ▽, $(\vec{e}_x, \vec{e}_y)$ plane and $R_\theta = 7\,500$; ♦, $(\vec{e}_z, \vec{e}_u)$ plane and $R_\theta = 7\,500$; □, $(\vec{e}_z, \vec{e}_u)$ plane and $R_\theta = 10\,500$; ▲, $(\vec{e}_z, \vec{e}_u)$ plane and $R_\theta = 13\,500$; ◯, $(\vec{e}_z, \vec{e}_u)$ plane and $R_\theta = 19\,000$; - - - - -, RMS spanwise vorticity; ———, Van Driest profile.

preferably tilted at more or less 45° downstream to the wall. The last interesting result in this region is the strong decrease toward the wall of the number of eddy structures of both sign detected in the $(\vec{e}_x, \vec{e}_y)$ plane indicating that the number of cane vortices is decreasing toward the wall, in favor of eddy structures forming small angles with the $(\vec{e}_x, \vec{e}_y)$ plane.

Mean Eddy Structures characteristics

Figures 3 and 4 show the mean radius and the mean vorticity profiles of the eddy structures at four Reynolds numbers in the $(\vec{e}_z, \vec{e}_u)$ plane and at $R_\theta = 7\,500$ in the $(\vec{e}_x, \vec{e}_y)$ plane. These two quantities appear relatively universal in wall units.

In the $(\vec{e}_z, \vec{e}_u)$ plane, the mean radius increases slowly away from the wall, starting from about 20^+ at $y^+ = 40$ and with a mean value of about 24^+ in the region of investigation. By contrast, the mean vorticity decreases slowly. The combination of both keeps the circulation (defined by $\langle\Gamma_o\rangle = 2\pi\langle\omega_o r_o^2\rangle$ in the case of an Oseen vortex) almost constant in wall units ($\langle\Gamma_o\rangle^+/2\pi = 140$). The mean vorticity profiles, extrapolated toward the wall, intersects the ω_z' profile around $y^+ = 25$, which corresponds to the peak of this quantity (the peak of ω_x' being nearby at $y^+ = 20$). At this wall distance, ω_z' is about two times the mean velocity gradient $\partial U/\partial y$ (which represents the main component of the mean vorticity). This supports the idea that the vortical structures observed further away from the wall have their origin around $y^+ = 25$, in the region of the strongest vorticity fluctuation, with an initial radius around 20^+ which places them just above the viscous sublayer.

In the $(\vec{e}_x, \vec{e}_y)$ plane, the size of the vortex heads is starting from the same near wall value. It slowly increases (almost linearly) with wall distance, leading to a slightly smaller mean value ($\sim 22^+$). The vorticity of the heads is slightly higher and remains significant away from the wall. The circulation is somewhat smaller ($\langle\Gamma_o\rangle^+/2\pi = 100$). It decreases slowly and linearly away from the wall. The results in the two other planes (not shown) agree well with those presented. Globally, one can conclude that the mean radius $\langle r_o\rangle^+$ of the vortices varies between 20 and 30 and increases slowly away from the wall while the mean circulation $\langle\Gamma_o\rangle^+/2\pi$ varies between 80 and 150 in the different planes and is almost constant (or very slowly linearly decreasing) through the region of observation.

The convection velocity (not shown), is very near to the mean velocity profile proposed by Van Driest. This result, which was already approached by a visualization study by Hoyez-Delaliaux (1990), is in good agreement with Adrian et al (2001). It has recently been confirmed by Christensen & Adrian (2002). The same results (not shown) is obtained in the $(\vec{e}_x, \vec{e}_y)$ plane together with a very good universality in wall units for $50 < y^+ < 500$ and for the four Reynolds numbers.

LOW AND HIGH SPEED STREAKS

The physical characteristics of the low and high speed streaks such as mean transverse spacing, and vertical and streamwise extent have been examined by various authors. For instance, Schraub & Kline (1965) initially established the mean spanwise spacing between low speed streaks ($\overline{\lambda}$) by using primarily flow visualization techniques for low Reynolds number flows ($R_e < 1500$). Thereafter, different measurements techniques were employed by numerous authors to determine this value (Kreplin & Echelmann (1979); Smith & Metzler (1983); Kahler (2004); and Carlier (2001)). It is generally accepted that $\overline{\lambda^+}=\overline{\lambda}u_\tau/\upsilon = 100 \pm 20$ for $y^+ \leq 10$ and increases for $y^+ \geq 10$. Nakagawa & Nezu (1981) suggested that the increase may be due to a pairing interaction of the low speed streaks as they move outward from the wall. It is also accepted that high speed streaks are a bit larger than low speed streaks (Carlier (2001) found 29 WU for the Low Speed Streaks (LSS) and 48 WU for the High Speed Streaks (HSS) at $y^+ = 15$ and $R_\theta = 7500$.) Blackwelder (1979), using a combination of hot film probes and flush mounted surface element in a low Reynolds number oil channel, found that the length of the low speed streaks can extend beyond 1000 wall units. Oldaker & Tiederman (1977), Kreplin & Echelmann (1979) and Carlier (2001) confirmed this result by their own experiments and agreed that the size of the low speed streak is between 500^+ and 2000^+ in length, and between 20^+ and 40^+ in width.

In the present study, specific measurements were performed in ten planes parallel to the wall in the buffer layer in order to characterize quantitatively the near wall streaks. Before looking for coherent structures, the statistical convergence of the PIV data was checked. The three diagonal terms of

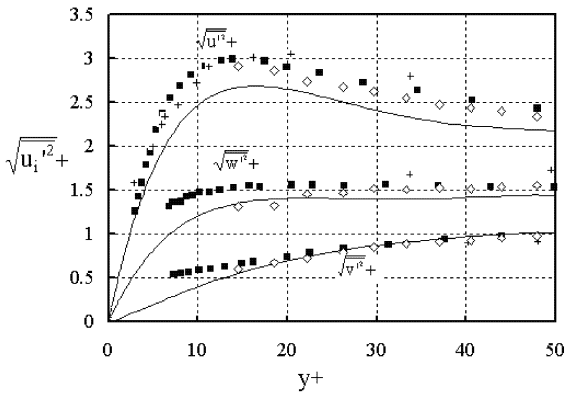

Figure 5: Turbulent statistics compared to HWA and DNS: ◇, PIV; ■, HWA; —-, DNS by Spalart (1988).

the Reynolds stress tensor were computed and compared to hot wire measurements and to the DNS results from Spalart (1988). The results are presented in figure 5. As can be seen, the agreement is fairly good between the three results. Very near the wall, the PIV data appear less affected by the in plane velocity gradient than the HWA by the wall interference.

To detect the streaks, the standard criterion based on the streamwise fluctuating velocity was used as an indicative function. This indicative function was thresholded at $u'/\sigma_u = 0.6$ in order to built a binary detection function. Digital image processing tools, based on Mathematical Morphology, were used in order to filter these detection functions (remove holes and small objects, smooth contours). Measurements in the transverse z direction were performed on these filtered images.

Figure 6 presents the statistical results obtained for the low and high speed streaks in the 10 PIV planes. The error bars has been estimated by varying the threshold between 0.5 and 1. The averaged width of the streaks varies almost linearly between 28 and 36 wall units for LSS and between 40 and 47 wall units for HSS. This is in good agreement with the results obtained by Carlier (2001) who observed comparable values and the same behavior with wall distance. The averaged distance between the streaks (from center to center of streaks) increases also with the wall distance but the behavior is not so smooth, especially for the HSS. The error bars are wider for the LSS than the HSS, showing more sensitivity to the threshold value. This indicates that the slope of the two types of object are different, the slope of the HSS being stronger. The distance obtained near the wall is in good agreement with the accepted values in the literature (Kreplin & Echelmann (1979); Smith & Metzler (1983); Kahler (2004); Carlier (2001)).

Figure 7 gives the probability density function of the LSS and HSS width at $y^+ = 15$ and 50. These distributions are far from gaussian, looking more like a Weibull law with an origin offset. Consequently, the most probable value is fairly different from the mean value for the LSS (20 and 28 respectively at $y^+ = 15$). At $y^+ = 15$, the LSS are obviously smaller than the HSS, both for the mean and the most probable value, but the range of both pdf is comparable. The HSS distribution is significantly wider than the LSS one. At $y^+ = 50$, the same tendency is observed for the mean values (see 6) but the most

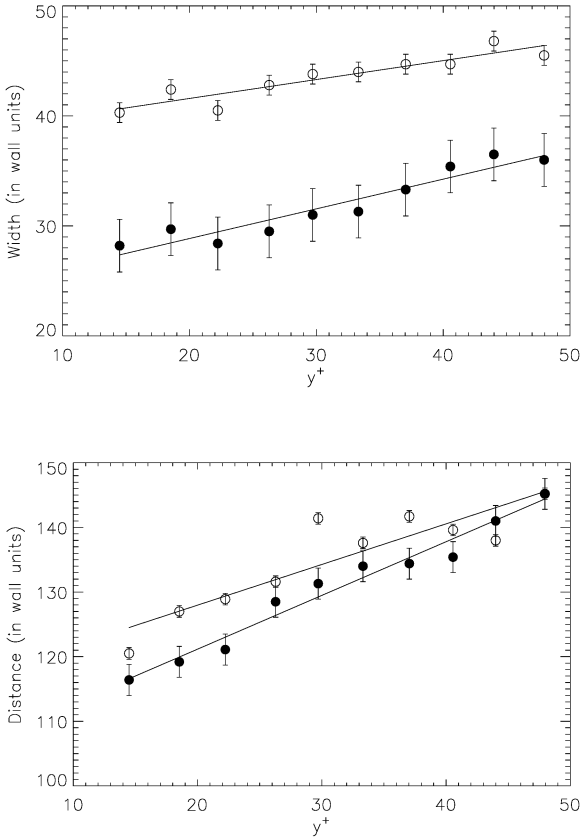

Figure 6: Mean characteristics of the low and high speed streaks. Top : streaks width, bottom : streaks distance, • LSS, ◯ HSS.

probable value is nearly the same (about 30 WU) and a bit smaller than the size of the vortices detected in this region ($D^+ \simeq 40$). Finally, it should be noticed that if the total number of both types of streaks is comparable at $y^+ = 15$, the LSS are obviously more numerous at $y^+ = 50$.

DISCUSSION AND CONCLUSION

Looking at the present results, one of the most significant ones is that all the physical characteristics of the detected vortices (size, intensity, convection velocity) in the logarithmic region seem to scale in wall units. The only contributors addressing this point in Panton (1997) are Hanratty & Papavassiliou (1997), who come to the same conclusion for both the size and the velocity scale of the vortices. Moreover, they obtained a size of $2r_o{}^+ \simeq 50$ near the wall, which is in fair agreement with the one found here.

A second interesting result concerns the characteristic scales of the eddy structures. Apart from near the wall, the vorticity of these eddies is much larger than the local mean shear stress ($\overline{U}_{x,y}$) and even the RMS of ω_z. This vorticity decreases very slowly away from the wall, while the size of the vortices increases, but also very slowly. The result is that the circulation of the eddies is nearly constant all through the region of observation which extends from the top of the buffer-layer to the middle of the logarithmic region ($y^+ \simeq 500$). A striking result is that this is true in all the planes of observa-

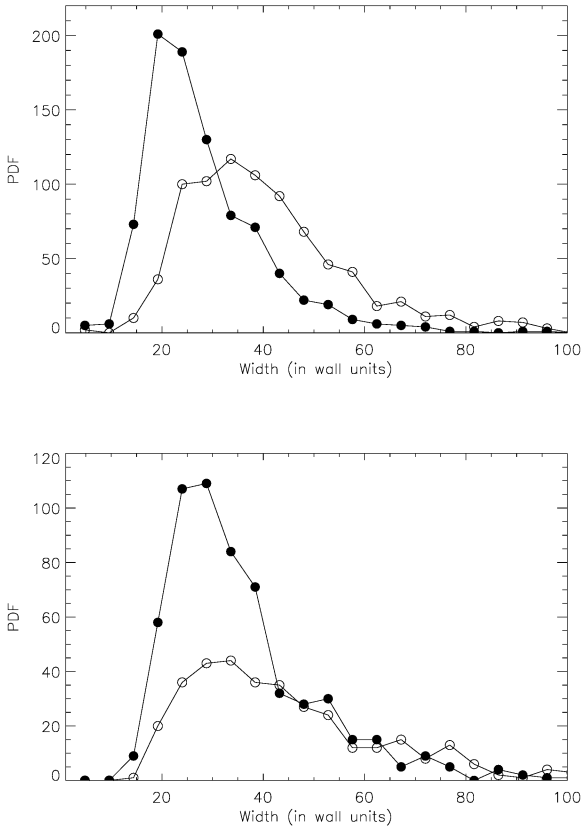

Figure 7: Probability density function of the width of the low and high speed streaks, top $y^+ = 15$, bottom $y^+ = 50$, • LSS, ◯ HSS.

tion, that is for both 'legs' and 'heads'. Also striking is the fact that these eddies seem to have the same origin: the near wall region around $y^+ = 25$, and a range of scale ${r_o}^+$ between 10^+ and 50^+ . These eddies are convected on average with the local mean velocity. They thus evidence little self-induction, being submitted mainly to the mean shear stress.

Looking at the Panton (1997) monograph, it is clear that the result about the scaling of the vortices is fairly contradicting to some well accepted ideas. Smith & Walker (1997), for example, are convinced that both hairpins and a majority of cane vortices travel near the wall in the outer part above the buffer-layer and send legs down toward the wall.

Hanratty & Papavassiliou (1997) come also to the conclusion that vortices grow significantly in size away from the wall (although the size they find near the wall is in fair agreement with the present result).

The contribution of Kline & Portela (1997) is mainly based on the well known analysis of the database of Spalart (1988) by Robinson (1991). They identify two families of vortices: tilted streamwise vortices near the wall (legs) and transverse vortices in the outer part (heads). Both are present in the logarithmic region and they are often connected on one side by a shoulder (very rarely on both sides $\sim 2\%$). They give no hint about the vortex size evolution away from the wall (see Robinson (1991)) but find a diameter of about 50^+ near the wall, in agreement with Hanratty & Papavassiliou (1997).

Schoppa & Hussain (2002) look in detail at the instability mechanism very near the wall in the buffer-layer, and give nearly no indication about the logarithmic region. They come to a model of staggered vortices of opposite sign riding over the low speed streaks and overlapping each other. These vortices are supposed to evolve rapidly into arches, through a streaks instability → streamwise vortices → arch vortices mechanism.

Apart from evident agreement with some results of each of these authors, the main contradiction between these results and the present data is the fact that the size of the vortices is proposed to grow rapidly as they move outward. Two main reasons can be put forward to explain this discrepancy. The first possible reason is that the present analysis may have missed the larger vortices due to the fact that they are not isotropic enough to fulfill the detection criterion. This reason is not supported by visual analysis of the data and also by the fact that Adrian et al (2001), using the same approach, come to a very similar estimation of the size of what they call the 'smallest' eddy structures. They also observe that this size is fairly constant throughout the BL. The second possible reason to explain this discrepancy is that most of the conclusions of the other authors, described above, rely mainly on the analysis of DNS or experimental data at fairly low Reynolds number, where the logarithmic region is very small (or even does not exist). This is not the case for the present data . If it can be confirmed that the size of the vortices increases in the wake region at high Reynolds number, then the contradiction may not be so strong between the present results and the existing data.

Summarizing the picture of eddy structures which emerge from the present data, one could say that the vortices in the logarithmic region are mainly canes of both sign, which scale in wall units. They find their origin near the wall, around $y^+ = 25$ and evolve initially mainly as tilted streamwise vortices. They keep their circulation and evolve very slowly with wall distance while being convected at the local mean velocity. The number of vortices found in each map indicates that they are fairly sparse in space, supporting somehow the hypothesis of active/inactive motions. Comparing this picture to a literature summary, it is clear that apart from the size evolution with wall distance, it is in fair agreement with most of them. This agreement is particularly good with the model developed by Schoppa & Hussain (2002).

It must finally be mentioned that, apart from the size, the picture obtained in the logarithmic region is in good agreement with the results of Christensen & Adrian (2002). The eddy structures appear to originate at the wall, to move slowly outward, while being convected downstream at the local mean velocity.

Concerning the near wall streaks, it appears that, although they are supposed to lay mostly in the viscous sublayer, both low and high speed streaks can be detected through out the buffer layer. The characteristic lengths obtained are in good agreement with the existing literature and appear to vary slowly with wall distance in this region. The PDFs of the widths are far from being gaussian, showing a significant skewness. They also evolve significantly with wall distance. It would be worth now to see how these streaks are associated with sweeps, ejections and streamwise vortices. This analysis is under way.

*

References

Adrian, R. J., Meinhart, C. D. & Tomkins, C. D., 2000, "Vortex organisation in the outer region of the turbulent boundary layer", J. Fluid Mech. **422**, 1–54.

Blackwelder, R. F. and Eckelmann, H., 1979, "streamwise Vortices associated with the bursting phenomenon", J. Fluid Mech **94**, 577–594

Carlier, J., 2001, "Étude des structures cohérentes de la turbulence de paroi à grand nombre de Reynolds par Vélocimétrie par Images de Particules", Thèse de Doctorat n^o 2959, Université des Sciences et Technologies de Lille, France.

Carlier, J., Stanislas, M., 2005, Experimental study of Eddy Structures in Turbulent Boundary Layer using PIV, *To appear in JFM.*

Christensen, K. T. & Adrian, R. J., 2002, "The velocity and acceleration signatures of small-scale vortices in turbulent channel flow", J. of Turbulence **3**.

Hama, F. R., 1954, "Boundary Layer Characteristics for Smooth and Rough Surfaces", Trans. Soc. Nav. Arch. Mar. Engrs **62**, 333.

Hanratty, T. J. & Papavassiliou, D. V., 1997, "The role of wall vortices in producing turbulence", *Self-Sustaining Mechanisms of Wall Turbulence*, (ed. R. L. Panton), Computational Mechanics Publications, 83–108.

Head, M. R. & Bandyopadhyay, P., 1981, "New aspects of turbulent boundary layer structure", J. Fluid Mech. **107**, 297–338.

Hoyez-Delaliaux, M. C., 1990, "Etude des caractéristiques instationnaires d'une couche limite turbulente de plaque plane sans gradient de pression", Thèse de Doctorat n^o 610, Université des Sciences et Technologies de Lille France.

Jie, L., Foucaut J. M., Laval J.P. et Stanislas M., 2004, "Optimisation de la PIV Stroscopique pour la caractrisation de la turbulence de paroi", *9ème Congrès Francophone de Vélocimétrie Laser, Bruxelles, 14-17 septembre 2004.*

Kähler, C. J. & Stanislas, M., 2000, "Investigation of wall bounded flows by means of multiple plane stereo PIV", *10th Int. Symp. on Appl. of Laser Tech. to Fluid Mech.*, Lisbon, Portugal.

Kahler, C. J., 2004, "Investigation of the spatio-temporal flow structure in the buffer region of a turbulent boundary layer by means of multiplane stereo PIV", Experiments in Fluids **36**, 114–130

Kim, H. T., Kline, S. J. & Reynolds, W. C., 1967, "The structure of turbulent boundary layers", J. Fluid Mech**30**,741–773

Kim, H. T., Kline, S. J. & Reynolds, W. C., 1971, "The production of turbulence near a smooth wall in a turbulent boundary layer", J. Fluid Mech **50**, 133–160

Kline, S. J. & Portela, L. M., 1997, "A view of the structure of turbulent boundary layers", in Self-Sustaining Mechanisms of Wall Turbulence, (ed. R. L. Panton), Computational Mechanics Publications, 167–180.

Kreplin, H. P. & Echelmann, H., 1979, "Propagation of pertubations in the viscous sublayer and adjacent wall region", J. Fluid Mech**59**,305–322

Nakagawa, H. & Nezu, I., 1981, "Structure of space time correlations of bursting phenomena in an open channel flow", J. Fluid Mech **104**, 1–43

Oldaker, o. K. & Tiederman, W. J., 1977, "Spatial structure of the viscous sublayer in drag-reducing channel flow", Phys. Fluid **20**, s133–144

Panton, R. L., 1997, "Self-Sustaining Mechanisms of Wall Turbulence", Computational Mechanics Publications.

Robinson, S. K., 1991, "Coherent motions in the turbulent boundary layer", Annu. Rev. Fluid Mech. **23**, 601–639.

Runstadler, P. C. & Kline, S.J. and Reynolds, W.C., 1963, Dept Mech. Engng, Stanford University, Rep *Trans. Soc. Nav. Arch. Mar. Engrs*,MD-8

Schoppa, W. & Hussain, F., 2002, "Coherent structure generation in near–wall turbulence", J. Fluid Mech. **453**, 57–108.

Smith, C. R. and Metzler, S.P., 1983, "The characteristics of low-speed streaks in the near-wall region of a turbulent boundary layer" J. Fluid Mech **129**, 27–54

Smith, C. R. & Walker, J. D. A., 1997, "Sustaining mechanisms of turbulent boundary layers: the role of vortex development and interactions", in Self-Sustaining Mechanisms of Wall Turbulence, (ed. R. L. Panton), Computational Mechanics Publications, 13–48.

Spalart, P. R., 1988, "Direct simulation of a turbulent boundary layer up to $R_\theta = 1410$", J. Fluid Mech. **187**, 61–98.

Schraub, F. A. & Kline, S. J., 1965, Dept Mech. Engng, Stanford University, Rep *Trans. Soc. Nav. Arch. Mar. Engrs*, MD-12

Theodorsen, T., 1952, "Mechanism of turbulence" Proc. Midwest. Conf. Fluid Mech., 2nd Edn, Colombus, Ohio, 1–18.